RSC Advances

ROYAL SOCIETY OF CHEMISTRY

www.rsc.org/advances

Flame retardant and toughening mechanisms of epoxy based on core-shell microspheres

Chunxia Zhao[1,2], Da He[2], Yi Wang[2], Yunliang Xing[2], Yuntao Li[1,2]*, Dong Xiang[2], Pengfei Lv[2]

[1] State Key Lab of Oil and Gas Reservoir Geology and Exploitation, Southwest Petroleum University, Chengdu 610500, People's Republic of China

[2] College of Material Science and Engineering, Southwest Petroleum University, Chengdu 610500, People's Republic of China

Abstract

Epoxy (EP) composites containing polystyrene-ammonium polyphosphate core-shell microspheres (CSP_{PS-APP}) were developed for flame retardant and toughening effects. The flame retardancy and thermal degradation behavior of the EP composites was investigated by limited oxygen index (LOI), vertical burning test (UL-94), cone calorimeter (CONE) and thermogravimetric analysis (TGA). Scanning electron microscope with energy-dispersive spectroscopy capability (SEM-EDS) was used to characterize the morphology and elements of the residual chars. A possible flame retardant mechanism of CSP_{PS-APP} in EP matrix was proposed based on the CONE, TGA and SEM-EDS results. The influence of CSP_{PS-APP} content on the glass transition temperature (T_g), storage modulus, Young's modulus, tensile strength and fracture toughness (K_{IC}) of material was also investigated. The results show that the CSP_{PS-APP} microspheres lead to significant flame retardant and char formation effects on the EP. The Young's modulus and fracture toughness of EP/CSP_{PS-APP} composites increase with increasing CSP_{PS-APP} content. The fracture toughness of the composite containing 15% CSP_{PS-APP} increased by approximately 59% compared to that of neat matrix. In addition, the critical strain energy release rate (G_{IC}) of the epoxy increased from 159 to 409 $J.m^{-2}$ with the addition of 15% CSP_{PS-APP}. The SEM images of fracture surface indicate that the enhanced toughness of EP/CSP_{PS-APP} composites can be attributed to the debonding of the core-shell

microspheres and the subsequent plastic void growth of the matrix, as well as the crack deflection effect of CSP_{PS-APP}.

Keywords: epoxy, core-shell microspheres, flame retardancy, fracture toughness

1. Introduction

Epoxy resin (EP) is one of the most commonly used thermosetting resins in composites industry. It is widely used as a matrix for structural complexes, as an encapsulating material for electronic devices and as adhesive or coating in aerospace industry [1-2]. These applications are mainly due to its high wetting ability, high chemical resistance and good mechanical properties (high Young's modulus and tensile strength) [3-5]. However, the brittleness and flammability of EP have restricted its further development in industrial applications.

Recently, many eco-friendly flame retardants have been developed to improve the flame retardancy of EP, involving phosphorous-, nitrogen-, silicon-, phosphorous-/nitrogen- containing compounds and inorganic nanofillers (montmorillonite and aluminum hydroxide et al.) [6-10]. Ammonium polyphosphate (APP) is a kind of phosphorous-/nitrogen- containing compounds, which has shown promising applications as a halogen-free flame retardant in EP. APP is useful to develop an effective flame retardant intumescent system due to its high phosphorus-nitrogen content. However, APP tends to migrate and bloom as a result of the poor compatibility with polymer matrices [11]. Microencapsulation and surface modification can markedly improve the water resistance and compatibility with polymeric materials of APP [11-14]. However, toughening polymer matrix is rarely taken into consideration in conventional modifications of APP. Inspired by microencapsulation mechanism, APP-poly (styrene) (PSt) core-shell microspheres were successfully synthesized *via in-situ* radical polymerization in our previous work [15]. Basic results of limiting oxygen (LOI) and vertical burning (UL-94) showed that the APP-PSt core-shell microspheres (CSP_{PS-APP}) exhibited good flame retardant effect on EP. Commonly, core-shell microspheres can provide toughness and reinforcement effects for thermosetting resins due to their special physical

structure [16].

The subject of this work is to evaluate the effect of APP-PSt core-shell microspheres on the flame retardant and toughening mechanism of EP. In our previous work, the authors found that the prepared APP-PSt core-shell microspheres increased the viscosity of the EP monomers and reduced the processability. To resolve this problem, diethyltoluenediamine (DETDA) which is stable above 100^{o}C at the presence of EP monomers was used as a curing agent in the current work. The EP system containing $CSP_{PS\text{-}APP}$ and DETDA was easy to be degassed and processed due to a lower viscosity relative to the previously reported system. In this work, we reported a remarkable improvement in the flame retardant and mechanical properties of EP with the incorporation of APP-PSt core-shell microspheres. The performance of APP-PSt core-shell microspheres as a multifunctional filler in EP system was evaluated by TGA, LOI, UL-94, CONE, DMA and single-edge-notch 3-point bend (SEN-3PB). Possible flame retardant and toughening mechanisms were proposed based on the SEM results of the char layer and fracture surface of EP/$CSP_{PS\text{-}APP}$ composites, respectively.

2. Experiment

2.1 Materials

Micro-sized polystyrene-ammonium polyphosphate core-shell spheres ($CSP_{PS\text{-}APP}$) were prepared by *in-situ* free-radical polymerization in our lab [15]. The mass percentage of the PS-APP microspheres shell is 49% as calculated by toluene extraction. The diameter of core-shell microspheres ranges from around 0.75 to 2.5 μm. The epoxy resin (Diglycidyl ether of bisphenol A, DGEBA) with an epoxide equivalent weight of 227 g/eq (E-44) was supplied by Wuxi Resin Factory of Blue Star New Chemical Materials Co., LTD (Jiangsu, China). The hardener, diethyltoluenediamine (DETDA), was provided by Chongshun Chemicals Co., LTD (Shandong, China).

2.2 Preparation of EP and flame retardant EP composites

Five grams of CSP_{PS-APP} microspheres were added into 79.0 g of epoxy (E-44) while stirring with a mechanical mixer for 20 min. Then 16.0 g of curing agent (DETDA) was added, and the mixture was heated to 100°C. In order to achieve a uniformly dispersed system, the mixture was stirred at 4000 RPM for 30 min and ultrasonicated for 40 min. The resin mixture was then degassed and poured into a preformed Teflon mold. The mixture was cured at 120°C for 2 h, 150°C for 2 h and 180°C for 2 h to produce EP/CSP_{PS-APP}-5% flame retardant composites. The neat EP and EP composites with 10 wt.%, 15 wt.% and 20 wt.% CSP_{PS-APP} were also prepared under the same processing conditions.

2.3 Characterization

Thermogravimetric analysis (TGA) was carried out using a NETZSCH TG 209 F1 instrument under air flow of 50 mL min^{-1}. The sample with a mass of 5.0 mg was heated from 40 °C to 700 °C at a heating rate of 20 °C min^{-1}.

The limited oxygen index (LOI) was measured on a HC-2C oxygen index meter (Jiangning, China) with sheet dimension of 130 mm × 3.5 mm × 3.2 mm, according to ASTM D2863-97. The vertical burning test for the U-L94 combustion level was performed on a CFZ-2-type instrument (Jiangning, China) according to the ASTM D3801 with sheet dimension of 125 mm × 12.7 mm × 3.2 mm. Cone calorimeter tests were performed with a UK device according to Fire Testing Technology (FTT) ISO 5660 at an incident flux of 35 kW/m^2. The specimen dimensions are 100 mm × 100 mm × (3.2±0.1) mm. The residual chars were imaged by a digital camera (Canon 6d) after testing.

The morphological and elemental analysis of the residual chars obtained was performed by a scanning electron microscope with energy-dispersive spectroscopy capability (SEM-EDS, JEOL JSM-5009LV) under an accelerating voltage of 5.0 kV. Prior to SEM morphology imaging, the residual chars were sputtered with thin layer of gold to provide conductive surfaces.

Dynamic mechanical analysis (DMA) for the specimens with dimensions of 40 mm × 10 mm × 3.2 mm was conducted at a fixed frequency of 1 Hz from 40 °C to 220 °C at a heating rate of 5 °C

min^{-1} using a RSA II (TA Instrument). Tensile properties of pure EP and flame retardant EP were measured according to ASTM D638-98 standard. The tensile tests were performed using an Instron universal material testing instrument at a crosshead speed of 5.0 mm min^{-1} at room temperature. At least five specimens were tested for each sample.

Fracture toughness tests were performed based on the linear elastic fracture mechanics (LEFM) approach at room temperature [17]. The mode-I critical intensity factor (K_{IC}) of pure EP and flame retardant EP was determined via single-edge-notch 3-point bend (SEN-3PB) tests according to ASTM-D5045-99. Five specimens for each sample were tested at a crosshead speed of 10 mm/min using a screw-driven mechanical testing machine (Instron Model 1125). K_{IC} was calculated by the equation (1) [18]:

$$K_{IC} = \frac{P \cdot S}{B \cdot W^{3/2}} \times f(\alpha/W) \quad (1)$$

where P is the load at crack initiation, S is the span width, B is the thickness of specimen, W is the width of specimen, α is the initial crack length, and $f(\alpha/W)$ is the geometry correction factor[19]. G_{IC} was calculated by the equation (2) [20]:

$$G_{IC} = \frac{\left(1-\upsilon^2\right) K_{IC}^{\ 2}}{E} \quad (2)$$

Where E is the Young's modulus and υ is the Poisson's ratio.

3. Results and discussion

3.1 Thermal properties of EP and EP/CSP_{PS-APP} composites

Thermal stability of pure EP and EP/CSP_{PS-APP} was investigated by TG and DTG under air atmosphere. The TG and DTG curves are shown in Fig.1 (a) and (b). The detailed data are summarized in Table 1. The initial decomposition temperature ($T_{initial}$) corresponding to 5% weight loss of pure EP appears at around 344 ^{o}C. Two maximum degradation rates, T_{max1} and T_{max2}, occur at 396 ^{o}C and 568 ^{o}C for the pure EP, and its char yield at 650 ^{o}C is 0.7% (Table 1). The incorporation

of CSP_{PS-APP} into EP facilitates the decomposition of EP in 300-450 °C, while it makes the residue weight ratio at 650 °C increase up to above 15.0%. With addition of 15% CSP_{PS-APP}, the $T_{initial}$ and T_{max1} of EP decreased to 332 °C and 349 °C respectively, and the char yield at 650 °C increased to 29.6%. The reason that the $T_{initial}$ of EP/CSP_{PS-APP} is lower than that of neat EP is mainly due to the decomposition of P=O and P-O bonds which have lower thermal stability than C-C bonds [21]. The mass loss at 500~650 °C is 24.2% for neat EP, 14.2% for EP/CSP_{PS-APP}-5%, and 7.0% for EP/CSP_{PS-APP}-10%. Moreover, the decreased $T_{initial}$ reflects a change of thermal decomposition behavior, in which more gas volatiles are generated from the initial degradation stage [22]. The chain scissions take place in the presence of relative unstable phosphorous-containing group at the early decomposition section of the EP matrix. With dehydration and carbonization, the phosphorous group acts as a promotion to form heat-resistant char, which can protect char from further oxidation degradation. The shell of CSP_{PS-APP}, polystyrene (PS), has near-zero char residue at high temperature [23]. Therefore, the excessive incorporation of CSP_{PS-APP} does not have a positive effect on the char formation. It can be observed in Table 1 that the residue amount of EP/CSP_{PS-APP}-20% is 3.1% lower than that of EP/CSP_{PS-APP}-15% at 650 °C. An appropriate phosphorous content can clearly lead to more efficient enhancement in the quantity of residues.

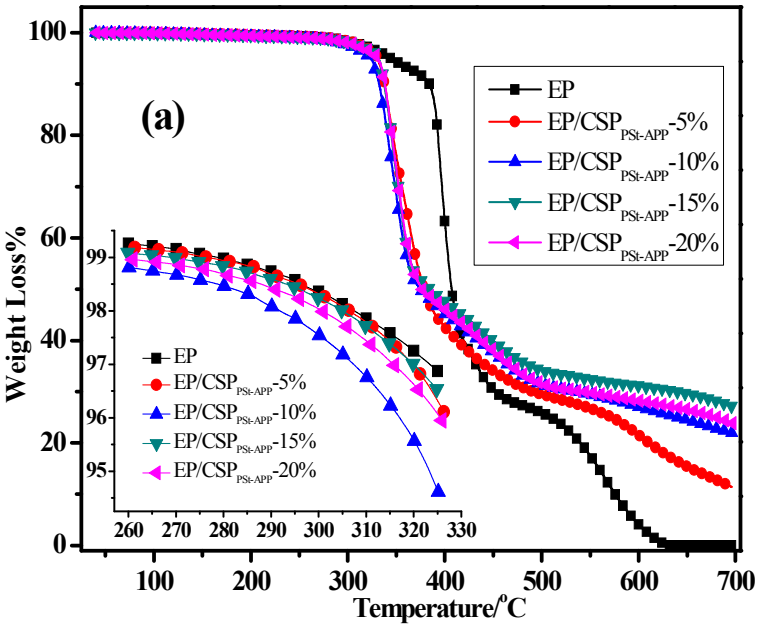

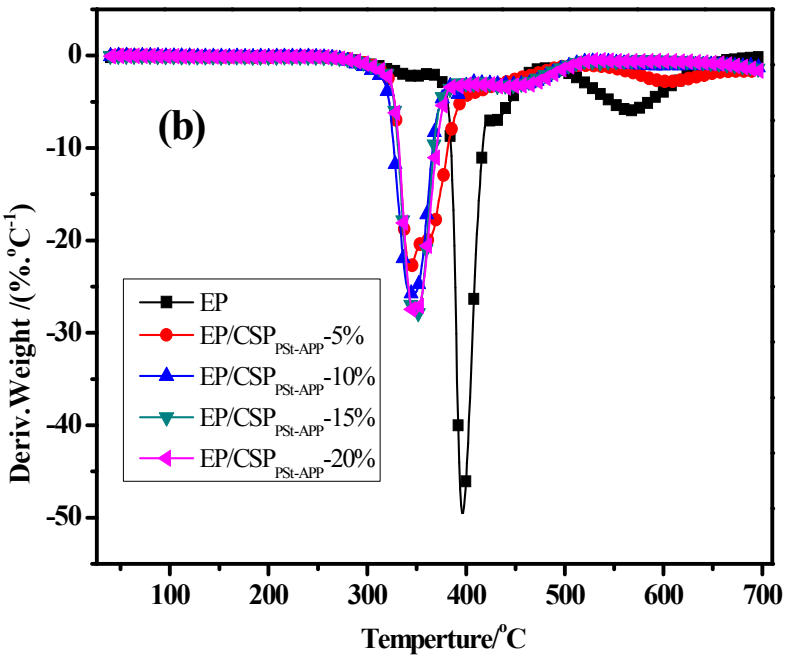

Fig. 1 TG (a) and DTG (b) curves of pure EP and EP/CSP_{PS-APP} composites at a heating rate of 20°C/min in air

Table 1 TG and DTG data of pure EP_{DETDA} and EP/CSP_{PS-APP} composites at a heating rate of 20°C/min in air

Sample	$T_{initial}$[a](°C)	T_{max1}[b] (°C)	T_{max2}[b](°C)	Char residue (%)	
				500 °C	650 °C
pure EP	344	396	568	25.9	0.7
EP/CSP_{PS-APP}-5%	330	350	603	29.5	15.3
EP/CSP_{PS-APP}-10%	324	347	--	31.5	24.5
EP/CSP_{PS-APP}-15%	332	349	--	34.2	29.6
EP/CSP_{PS-APP}-20%	330	348	--	31.6	26.5

3.2 Flame retardancy

The influence of CSP_{PS-APP} microspheres on the flame retardancy of EP was investigated by UL-94 vertical testing and LOI. The results of LOI and UL-94 test are shown in Table 2. The flame retardancy of the EP resins was significantly improved with the incorporation of CSP_{PS-APP}. No char

layer formed for neat EP during the LOI and UL-94 testing. The thermally decomposing surface was exposed directly to fire and propagated quickly to the fixture. Therefore, no UL-94 rate (NR) is observed for pristine EP. LOI value is 26.0 for EP/CSP_{PS-APP}-5% and dripping is no longer observed. For EP composites loaded with 5% and above of CSP_{PS-APP}, self-extinguishing can be measured and the burning time are significantly decreased. According to UL-94 test results, the second burning times (t_2) of EP composites with 5-20 % of CSP_{PS-APP} are extremely shorter than the first ones (t_1). It can conclude that the effective protection of char layer formed on EP/CSP_{PS-APP} composites during the first combustion section. EP/CSP_{PS-APP}-15% has the highest LOI value and best flame retardant properties, which is probably attributed to the effect match of acid, charring and gas sources for intumescent char formation.

Table 2 LOI and UL-94 test results of EP and EP/CSP_{PS-APP} composites

Sample	LOI	UL-94	t_1 (s)	t_2 (s)
pure EP	22.5	NR	---	---
EP/CSP_{PS-APP}-5%	26.0	V-1	36	26
EP/CSP_{PS-APP}-10%	27.6	V-1	24	17
EP/CSP_{PS-APP}-15%	29.7	V-1	9	6
EP/CSP_{PS-APP}-20%	28.8	V-1	15	9

The flame retardancy of the EP resins was significantly improved with the incorporation of CSP_{PS-APP}. The fire safety properties of EP and EP/CSP_{PS-APP} composites, including the heat release rate (HRR) and CO_2 yield, are shown in Fig. 2 and Fig. 3. The peak of heat release rate (PHRR) of EP significantly decreases with the addition of CSP_{PS-APP} microspheres in the matrix. Compared to the neat EP, the PHRR of EP/CSP_{PS-APP}-5% clearly decreased from 1128 kW/m^2 to 718 kW/m^2. Interestingly, the EP/CSP_{PS-APP}-15% exhibited the lowest PHRR among all the samples, which

decreased by 57% compared to the pure EP. The PHRR of EP/CSP_{PS-APP}-20% is 22% higher than that of EP/CSP_{PS-APP}-15%, which is agree with the results of LOI and UL-94 test. The matching of acid, charring and gas sources is the key factor to form a good quality intumescent charring layer [24]. For EP/CSP_{PS-APP}-5% and EP/CSP_{PS-APP}-10%, the generated volatile gases escaped before forming charring layer and could not play an effect role in the intumescent state. In case of EP/CSP_{PS-APP}-20% composites, pimping holes were observed on the outside surface of char layer because of the low viscosity of thermal degraded soften mixture. These phenomena can be firmly confirmed by the digital and SEM images of the char layer formed during the cone calorimeter test and will be discussed in the following sections. According to the above discussion on TGA data and the following morphology of char residuals, the EP/CSP_{PS-APP}-15% shows the most efficient reinforcement in the fire safety properties of EP, which is probably attributed to the condensed char layer as shown in Fig . 4.

Fig. 3 presents the results of CO_2 production (CO_2P) of EP and its composites. It can be seen in Fig. 3 that the CO_2 production of samples decreases with the incorporation of CSP_{PS-APP}, indicating that the CSP_{PS-APP} can reduce the flammability and toxic gas emission of EP. Lower CO_2P suggests that more residual mass remains during testing. The CO_2 emission is resulted from the evolution of complete-oxidation products. The maximum CO_2P rates of EP/CSP_{PS-APP}-5%~20% decreased by 37%~60% compared to that of neat EP. The enhanced incomplete combustion for the EP/CSP_{PS-APP} composites can be mainly attributed to the generation of a protective char layer.

The time to ignition (TTI) is used to determine the effect of CSP_{PS-APP} on ignitability, which can be measured from the onset of HRR curves. Ignition occurs when the volatiles are sufficient to be ignited by a spark [25]. It can be observed in Fig. 2 and Fig. 3 that the EP/CSP_{PS-APP}-5% and EP/CSP_{PS-APP}-10% release heat and CO_2 earlier than the neat EP, indicating a decreased TTI. The decrease in the TTI of EP/CSP_{PS-APP}-5% and EP/CSP_{PS-APP}-10% is mainly due to the highly production of volatile products released in the initial decomposition of CSP_{PS-APP} and EP matrix

before they facilitates the char formation. Contrarily, an increase in TTI was detected clearly for the EP/CSP_{PS-APP}-15% and EP/CSP_{PS-APP}-20%. During heating or combustion, APP in CSP_{PS-APP} microspheres can decompose to form poly(phosphoric acid) accompanying with ammonia [24]. The phosphate ester may undergo a cross-linking reaction with EP matrix or itself to promote an intumescences char formation, during which processes much water is generated. Proper incorporation of CSP_{PS-APP} results in enough ammonia and water, which can dilute the concentration of the combustible gases, leading to the delay of TTI for EP/CSP_{PS-APP}-15% and EP/CSP_{PS-APP}-20% composites. In addition, the accelerated and effective formation of intumesce char layer on the surface is also helpful to increase the TTI.

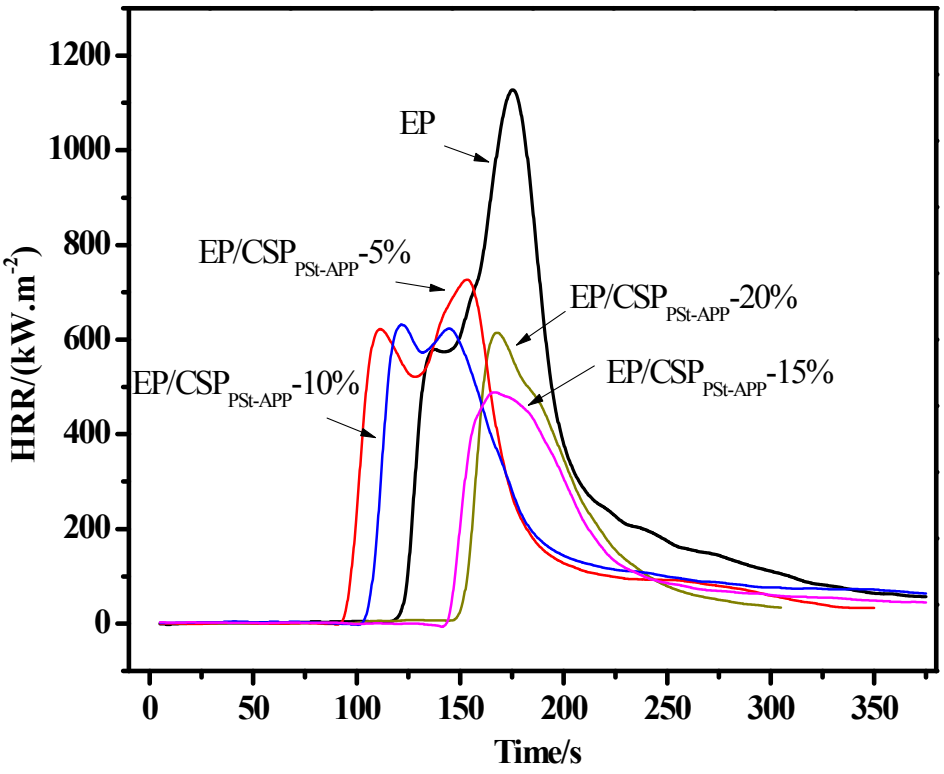

Fig. 2 Heat release rate curves of EP and EP/CSP_{PS-APP} composites

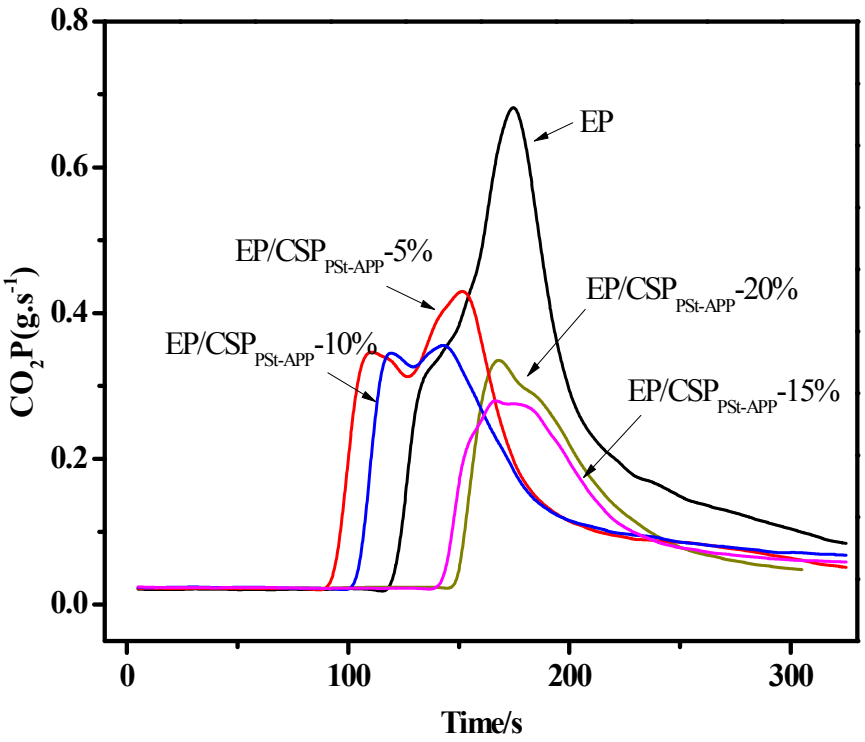

Fig. 3 CO_2 production rate of samples with time

3.3 Morphology and EDS of the residual char

The digital photographs and SEM images of the residual char layers from the CONE tested EP and EP/CSP_{PS-APP} composites are shown in Fig. 4 and Fig. 5, respectively. There is no obvious char formation for the neat EP. However, the char layers for the EP/CSP_{PS-APP} composites are intumescent and firm. Interestingly, it can be observed in Fig. 4 that the char layer of EP/CSP_{PS-APP}-15% composite is expanded the most in volume. This suggests that a proper incorporation of CSP_{PS-APP} is critical for the formation of high quality char layer. The outside surface of the char layer of EP/CSP_{PS-APP}-15% is compact enough to prevent gas penetration and to cut off oxygen from the degraded volatiles efficiently. The inner structure of the char of EP/CSP_{PS-APP}-15% is bumpy and porous (Fig. 5b). Small holes were observed on the outer surface of EP/CSP_{PS-APP}-20% char layer, see as the arrows in Fig. 5c. Moreover, the numbers of small bubbles in the inner structure of EP/CSP_{PS-APP}-20% (Fig. 5d) is obvious less than that in the internal char of EP/CSP_{PS-APP}-15%. These factors confirm the importance of matching of acid, charring and gas sources for the high quality intumescent char formation. As a result, compared with EP/CSP_{PS-APP}-20% composite,

EP/CSP_{PS-APP}-15% has a better quality intumescent char corresponding to a higher LOI value, a lower HRR, and better flame retardant properties. The air trapped in the microporous structure can reduce the efficiency of heat transfer. Generally, the intumescent char layer could slow down the heat and mass transfer between the gas and solid phases, so it can provide better flame shield for the underlying material during combustion [26-27].

The concentrations of C, O, N and P in the char of EP/CSP_{PS-APP}-15% were investigated by EDS. The EDS results are summarized in Table 3. One can see that the main elements of both the outside and inside of char are C. This result indicates that the CSP_{PS-APP} can reserve more C atoms in the EP residual to form a carbon-rich char layer. The ratio of O content in the outside surface to that of the inner structure is 1.5. This demonstrates a better antioxidation of inner matrix arising from the protection of compact and continuous outside surface. A higher P content in the outside surface of the char can be detected compared to the inner structure, which is mainly attributed to the migration of CSP_{PS-APP} from the inner side to the surface of matrix. The main reason for the formation of this kind of char will be discussed in the following section.

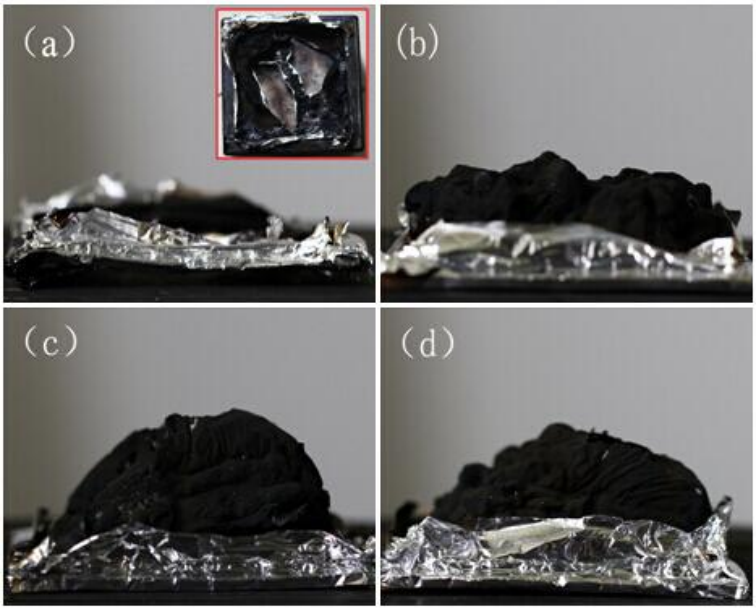

Fig. 4 Digital morphologies of chars from EP and EP/CSP_{PS-APP} composites after CONE test. (a) pure EP, (b) EP/CSP_{PS-APP}-10%, (c) EP/CSP_{PS-APP}-15% and (d) EP/CSP_{PS-APP}-20%

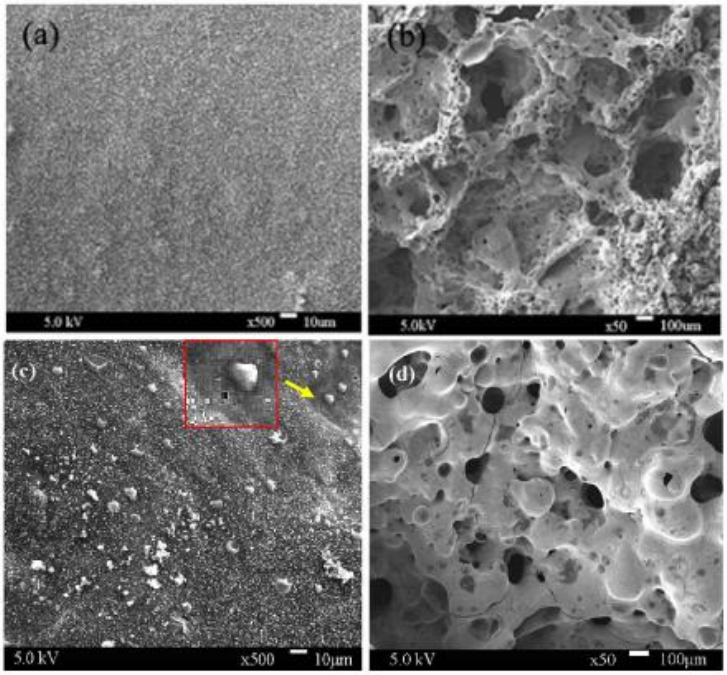

Fig. 5 SEM morphologies of char from the CONE tested. (a) outside surface and (b) inner structure of EP/CSP_{PS-APP}-15%; (c) outside surface and (d) inner structure of EP/CSP_{PS-APP}-20%.

Table 3 EDS results of residue for the EP/CSP_{PS-APP}-15% composite

Elements	Outside surface		Inner structure	
	Weight ratio/%	Atom ratio/%	Weight ratio/%	Atom ratio/%
C	61.18	68.48	77.05	82.82
O	11.07	10.63	7.39	6.82
N	21.83	18.34	10.08	8.14
P	5.68	2.47	4.94	2.06

3.4 Possible flame retardant mechanism of CSP_{PS-APP} in EP

Based on the experimental data above, a possible flame retardant mechanism of CSP_{PS-APP} in EP matrix is proposed (Scheme 1). The combustion of EP resin can be described as the following processes. The decomposition of EP initiates when it is heated to a certain onset temperature with some flammable gases generated in the reaction with oxygen. A large amount of heat which can

further promote the degradation of matrix is released in the combustion process until the EP is bunt out. In terms of the EP/CSP_{PS-APP} composites, the CSP_{PS-APP} will migrate to the surface of composites and aggregate with the aid of heat and gas flow in the soften EP matrix when the composites are exposed to fire or flame (Scheme 1 a). Then, the PS shell is melted and mixed with the soften EP to form a viscous mixture (Scheme 1 b). The melted PS covered on the composite surface undergoes thermal degradation with the release of PS· and H· [28]. The subsequent reaction between the radicals and oxygen leads to the degradation of matrix. It is well known that the phosphorus containing flame retardant reagent can accelerate the degradation reaction of polymer materials. In these cases, hydrogen atom abstraction from α-position of PS produces a chain radical on the polymer [29], which consequently induces a flaming combustion. In the EP/CSP_{PS-APP} composites, the uncovered APP is thermally decomposed to form poly (phosphoric acid), which can cross-link with PS during combustion. The poly (phosphoric acid) dehydrates the hydroxyl groups in EP resulting in the formation of a three dimensional cross-linked network structure during the preliminary decomposition (Scheme 1 c). The phosphate ester bonds in poly (phosphoric acid) will be broken down earlier than the common C-C or C-O bonds in PS or EP to generate the phosphoric acid due to their less stability. These results in an increase in the viscosity of melt mixture during pyrolysis and combustion. The ammonia, water and molecule fragments released in the pyrolysis process of APP, EP and PS acts as the gas source to plump up the melted-vitresence surface [22, 24, 28]. The intumescent char layer is then formed to protect the matrix material effectively (Scheme 1 d). As described above, the enhanced flammability properties of EP/CSP_{PS-APP} composites can be mainly attributed to the solid phase flame retardant mechanism. The CSP_{PS-APP} microspheres can promote the formation of compact char layer in the solid phase of composite matrix during combustion. Therefore, the control of heat transfer and the reduction in volatiles amount are very important in the improvement of flame retardant properties of polymers [30].

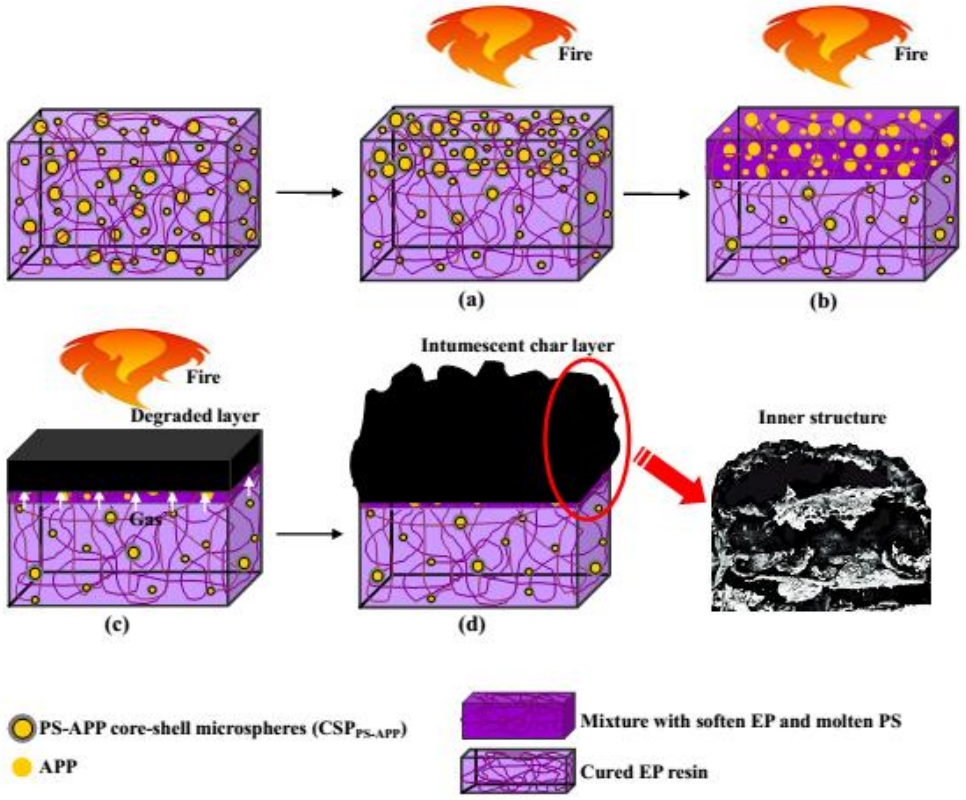

Scheme 1 Possible mechanism of char formation during the combustion of EP/CSP$_{PS-APP}$ composites

3.5 Thermal dynamic mechanical properties

The effectiveness of CSP$_{PS-APP}$ microspheres in improving the flame retardancy of EP has been demonstrated based on the results above. Clearly, a non-halogen method to enhance the flame retardancy of polymers without sacrificing other properties, such as glass transition temperature (T_g), mechanical properties and fracture toughness, is very attractive to academic and industrial communities.

The DMA results are shown in Fig. 6 and Fig. 7. A single glass transition peak is observed in the dynamic mechanical spectrum of EP and its composites. The neat EP shows a T_g at 171^{o}C. The T_g of EP decreases slightly with the addition of 5% and 10% CSP$_{PS-APP}$ microspheres mainly due to an under-curing of EP matrix. However, the EP/CSP$_{PS-APP}$-15% shows a T_g of 173^{o}C. It is clear that the T_g of EP/CSP$_{PS-APP}$ composites depend on a balance between the confinement effect of CSP$_{PS-APP}$ and its influence on curing reaction. The presence of microspheres can cause the under-curing of the

EP matrix, while they can also act as the barriers to reduce the mobility of chain segments. It can be assumed that the confinement effect dominates this relationship in the EP/CSP_{PS-APP}-15%, therefore the EP/CSP_{PS-APP}-15% has a slightly higher T_g compared to the neat EP.

The CSP_{PS-APP} microspheres exhibit different effects on the storage modulus of EP at the temperatures above and below T_g. The storage modulus of EP increases at glassy state with the addition of 5% and 10% CSP_{PS-APP}, while it decreases at rubbery state. The decreased storage modulus of EP/CSP_{PS-APP}-5% and EP/CSP_{PS-APP}-10% is mainly caused by the lower crosslink density of EP. However, the storage modulus increases with the addition of 15% CSP_{PS-APP} at both glassy and rubbery state, compared to the pure EP. It indicates that the chain segments of EP could be restricted severally when a higher CSP_{PS-APP} content is added in the composites.

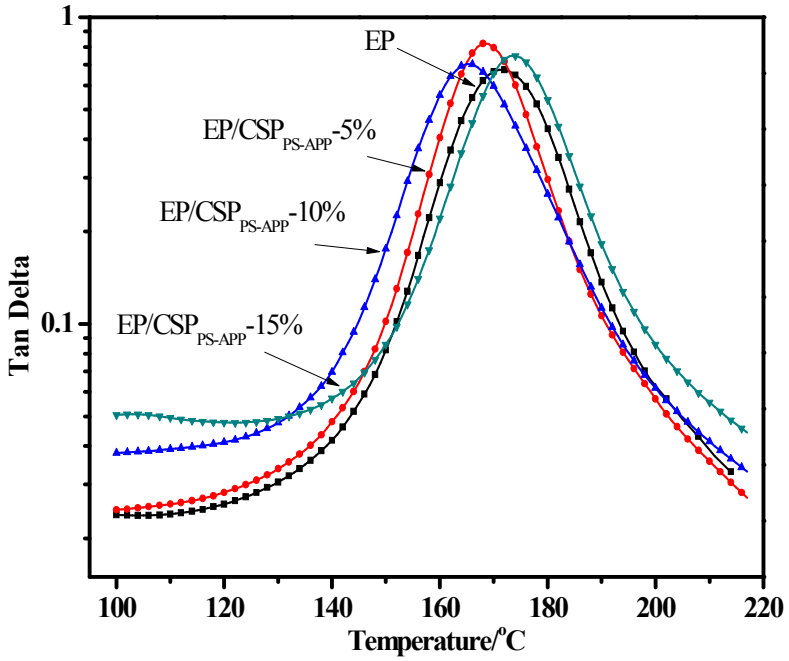

Fig. 6 Tg of the EP and EP/CSP_{PS-APP} composites.

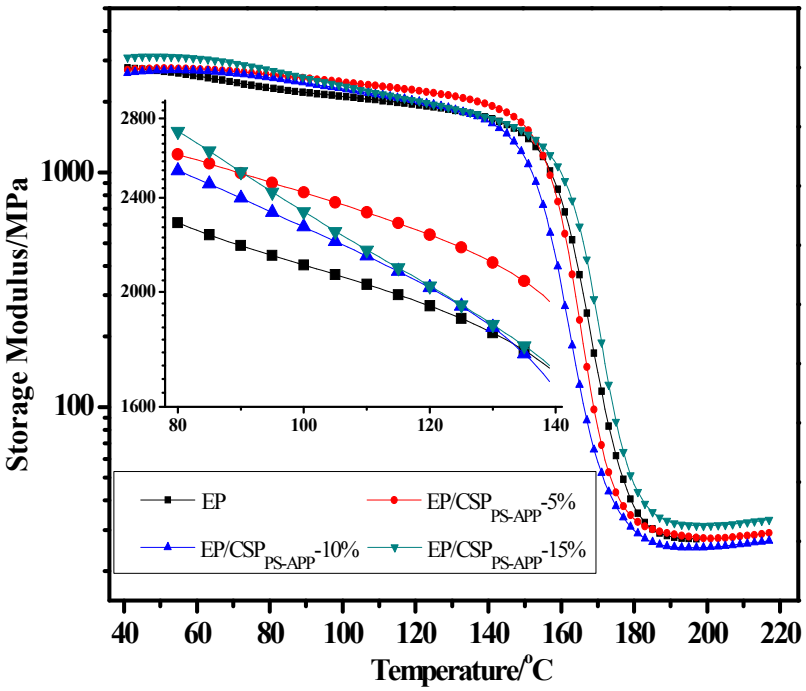

Fig. 7 Storage modulus of the EP and EP/$CSP_{PS\text{-}APP}$ composites.

3.6 Tensile and fracture toughness properties

The tensile and fracture toughness properties of the EP and composites were also investigated in this work. The typical stress-strain curves of the neat EP and EP/$CSP_{PS\text{-}APP}$ composites are shown in Fig. 8. One can see that both the neat EP and EP/$CSP_{PS\text{-}APP}$ systems present a typical brittle behavior, where the plastic deformation is absent prior to failure due to the original brittleness of EP. The tensile strength and elongation of material increase with the addition of 5% and 10% $CSP_{PS\text{-}APP}$. Compared with the neat EP, the elongation of EP/$CSP_{PS\text{-}APP}$-15% decreased from 10.1% to 7.3%. The Young's modulus of the neat EP and EP/$CSP_{PS\text{-}APP}$ composites was calculated from the linear region of stress-strain curves and plotted as a function of $CSP_{PS\text{-}APP}$ loading in Fig. 9. The neat EP shows a Young's modulus of 2687 MPa. It is found that the modulus increases with increasing $CSP_{PS\text{-}APP}$ content. The Young's modulus increased to approximately 3100 MPa for the 10% $CSP_{PS\text{-}APP}$ modified epoxy. Also, the fracture toughness (K_{IC}) and critical strain energy release rate (G_{IC}) of the epoxy increases with the addition of more $CSP_{PS\text{-}APP}$ (Table 4). The K_{IC} increased from 0.70

MPa.m$^{1/2}$ for the pure EP to approximately 1.11 MPa.m$^{1/2}$ for EP/CSP$_{PS-APP}$-15% composite. The G_{IC} of the composite containing 15% CSP$_{PS-APP}$ increased by 157% compared to that of neat matrix.

In order to better understand the effect of CSP$_{PS-APP}$ on the mechanical properties of EP, the crack tip regions of fracture surfaces of EP and EP/CSP$_{PS-APP}$ composites were investigated by SEM. The SEM images of samples are shown in Fig. 10. It can be observed in Fig. 10a that the neat epoxy shows a nearly featureless fracture surface without any deviation in crack growth, which is typical for a brittle thermosetting resin. Besides, there is no large-scale plastic deformation during fracture. This agrees with the low fracture toughness of pure EP (Table 4). With the addition of CSP$_{PS-APP}$, numerous crack steps occur during the propagation of cracks, indicating the localized crack deflection and crack bifurcation (Fig. 10 b, c and d). The CSP$_{PS-APP}$ particles show a pinning effect on inhibiting the propagation of cracks, which force the cracks to bow out and around the particles. As a result, significant fracture energy can be dissipated by this manner [31]. Debonding and void growth between the CSP$_{PS-APP}$ particles and EP matrix are clearly observed on the fracture surfaces for all the EP/CSP$_{PS-APP}$ systems. This can be more likely explained as that the increase in plastic zone generated by the CSP$_{PS-APP}$ changes the stress state around the microspheres and the increased triaxial tension facilitates debonding and subsequent void growth. The increased fracture toughness of the EP/CSP$_{PS-APP}$ composite systems can be supported by this toughening mechanism.

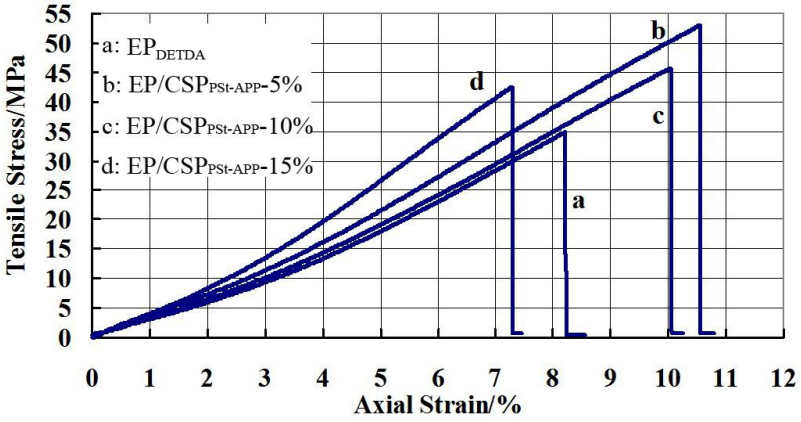

Fig. 8 Strain-stress curves of the EP and EP/CSP$_{PS-APP}$ composites.

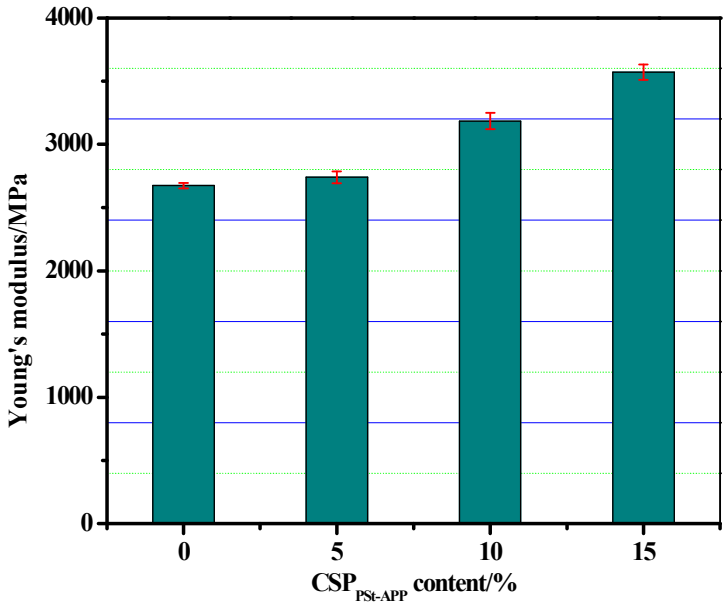

Fig. 9 Young's modulus of epoxy composites as a function of $CSP_{PS\text{-}APP}$ content.

Table 4 K_{IC} and G_{IC} of the EP and $CSP_{PS\text{-}APP}$ composites.

Sample	K_{IC}/MPa.m$^{1/2}$	G_{IC}/J.m^{-2}
EP	0.70±0.04	159±18
EP/$CSP_{PS\text{-}APP}$-5%	0.81±0.02	179±27
EP/$CSP_{PS\text{-}APP}$-10%	0.93±0.03	236±22
EP/$CSP_{PS\text{-}APP}$-15%	1.11±0.05	409±31

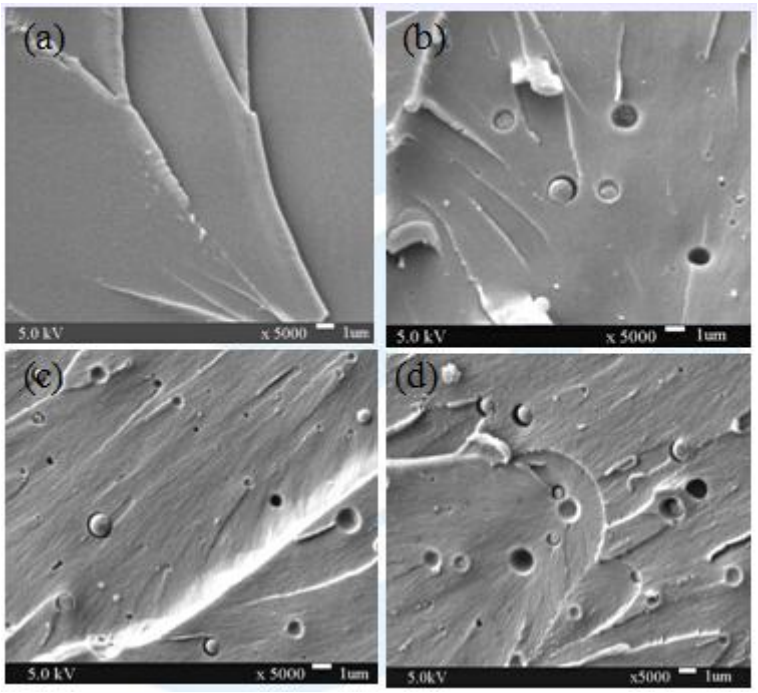

Fig. 10 SEM images of fracture surface of the tensile tested EP and EP/CSP composites. a, EP; b, EP/$CSP_{PS\text{-}APP}$-5%; c, EP/$CSP_{PS\text{-}APP}$-10%; d, EP/$CSP_{PS\text{-}APP}$-15%.

4. Conclusions

$CSP_{PS\text{-}APP}$ microspheres have significant flame retardant and toughening effects on epoxy. CONE and TGA analysis indicate that the enhancement in the flame retardant property of EP is resulted from the high weight ratio of char residual. The char residue has a honeycomb structure with compact surface, which works as an effective barrier for the transportation of oxygen, flame and polymer matrix. Compared to the neat EP, the PHRR of EP/$CSP_{PS\text{-}APP}$-15% decreased clearly from 1128 kW/m^2 to 487 kW/m^2, while the T_g of EP/$CSP_{PS\text{-}APP}$-15% was barely influenced. The experimental results on the mechanical properties of material demonstrate that the EP can be toughened by the $CSP_{PS\text{-}APP}$. The K_{IC} and G_{IC} of composites are significantly enhanced with the addition of $CSP_{PS\text{-}APP}$. A possible toughening mechanism involving debonding, crack deflection and void growth is proposed based on the SEM analysis of fracture surface of samples. This study indicates that the $CSP_{PS\text{-}APP}$ can act as an excellent multifunctional modifier to enhance the flame retardancy and toughness of EP significantly.

Acknowledgments

The work was financially supported by the Scientific Research Starting Project (No. 2014QHZ019), the Innovation Fund for Postgraduates (CXJJ2015005) and the Foundation for the Key Lab of Oil and Gas Material of Southwest Petroleum University (No. X151515KCL38), China.

References

[1] Wang YZ, Zhao JQ, Yuan YC, Liu SM, Feng ZM, Zhao Y. Synthesis of maleimido-substituted aromatic s-triazine and its application inflame-retarded epoxy resins. Polym Degrad Stabil 2014; 99:27-34.

[2] Qian LJ, Ye LJ, Xu GZ, Liu J, Guo JQ. The non-halogen flame retardant epoxy resin based on a novel compound with phosphaphenanthrene and cyclotriphosphazene double functional groups. Polym Degrad and Stabil 2011;96(6):1118-1124.

[3] Liu QH, Zhou XF, Fan XY, Zhu CY, Yao XY, Liu ZP, et al. Mechanical and Thermal Properties of Epoxy Resin Nanocomposites Reinforced with Graphene Oxide. Polym-Plast Technol 2012;51(3): 251-256.

[4] Rafiee MA; Rafiee J; Wang Z; Song HH; Yu ZZ; Koratkar N. Enhanced Mechanical Properties of Nanocomposites at Low Graphene Content. ACS Nano 2009;3(12):3884-3890.

[5] Zhang HB, Zheng WG, Yan Q, Yang Y, Wang JW, Lu ZH, Ji GY, Yu ZZ, et al. Electrically conductive polyethylene terephthalate/graphene nanocomposites prepared by melt compounding. Polymer 2010;51(5):1191-1196.

[6] Liu WS, Wang ZG, Xiong L, Zhao LN. Phosphorus-containing liquid cycloaliphatic epoxy resins for reworkable environment-friendly electronic packaging materials. Polymer 2010;51(21): 4776-4783.

[7] Toldy A, Szolnoki B, Marosi G. Flame retardancy of fibre-reinforced epoxy resin composites for aerospace applications. Polym Degrad Stabil 2011;96(3):371-376.

[8] Toldy A, Toth N, Anna P. Synthesis of phosphorus-based flame retardant systems and their use in

an epoxy resin. Polym Degrad Stabil 2006;91(3):585-592.

[9] Das G, Karak N. Vegetable oil-based flame retardant epoxy/clay nanocomposites. Polym Degrad Stabil 2009;94(11);1948-1954.

[10] Raimondo M, Russo S, Guadagno L, Longo P, Chirico S, Maricond A, Bonnaud L, Murariu O, Dubois P, et al. Effect of incorporation of POSS compounds and phosphorous hardeners on thermal and fire resistance of nanofilled aeronautic resins. RSC Adv 2015;5(15):10974-10986.

[11] Lu SF, Xing JW, Zhang ZH, Jia GP. Preparation and characterization of polyurea/polyurethane double-Shell microcapsules containing butyl stearate through interfacial polymerization. J App Polym Sci 2011;121(6):3377-83.

[12] Essawy H, Tauer K. Polyamide capsules via soft templating with oil drocps-1. Morphological studies of the capsule wall. Colloid Polym Sci 2010;288(3):317-31.

[13] Giraud S, Bourbigot S, Rochery M, Vroman I, Tighzert L, Delobel R, et al. Flame behavior of cotton coated with polyurethane containing microencapsulated flame retardant agent. J Ind Text 2011; 31(1):11-26.

[14] Giraud S, Bourbigota S, Rochery M, Vroman I, Tighzert L, Delobel R,et al. Microencapsulation of phosphate: application to flame retarded coated cotton. Polym Degrad Stab 2002; 77(2):285-97.

[15] Zhao CX, Li YT, Xing YL, He D, Yue J. Flame Retardant and Mechanical Properties of Epoxy Composites Containing APP-PSt Core-Shell Microspheres. J Appl Polym Sci. 2014;131(9):40218-40225.

[16] Giannakopoulos G, Masania K, Taylor AC. Toughening of epoxy using core–shell particles. J Mater Sci 2011; 46(2):327-338.

[17] Sun L, Warren GL, O'Reilly GY, Everett WN, Lee SM, Davis D, Lagoudas D, Sue HJ, et al. Mechanical properties of surface-functionalized SWCNT/epoxy composites. Carbon

2008;46(2):320-328.

[18] Liu J, Sue HJ, Thompson ZJ, Bates FS, Dettloff M, Jacob G, Verghese N, Pham H, et al. Nanocavitation in Self-Assembled Amphiphilic Block Copolymer-Modified Epoxy. Macromolecules 2008;41(20):7616-7624.

[19] S. G. Tan and W. S. Chow, Thermal Properties, Fracture Toughness and Water Absorption of Epoxy-Palm Oil Blends, Polym-Plast Technol 2010;49(9):900-907.

[20] Hamerton I, McNamara LT, Howlin BJ, Smith PA, Cross P, Ward S, et al. Toughening Mechanisms in Aromatic Polybenzoxazines Using Thermoplastic Oligomers and Telechelics. Macromolecules 2014; 47(6): 1946-1958.

[21] Hu Z, Chen L, Zhao B, Luo Y, Wang DY, Wang YZ. A novel efficient halogen-free flame retardant system for polycarbonate. Polym Degrad Stabil 2011;96(3): 320-327.

[22] He QL, Yuan TT, Wei SY, Guo ZH. Catalytic and synergistic effects on thermal stability and combustion behavior of polypropylene: influence of maleic anhydride grafted polypropylene stabilized cobalt nanoparticles. J Mater Chem A 2013; 1, 13064-13075.

[23] Muraki T, Ueta M, Ihara E, Inoue K. Enhancement of thermal stability of polystyrene and poly(methyl methacrylate) by cyclotriphosphazene derivatives. Polym Degrad and Stabil 2004;84(1):87-93.

[24] Gu JW, Zhang GC, Dong SL, Zhang QY, Kong Jie. Study on preparation and fire-retardant mechanism analysis of intumescent flame-retardant coatings. Surface & Coatings Technology 2007; 201(18):7835-7841.

[25] Zhang W, Li X, Yang R. Novel flame retardancy effects of DOPO-POSS on epoxy resins. Polym Degrad and Stabil 2011;96(12):2167-2173.

[26] Jian RK, Chen L, Chen SY, Long JW, Wang YZ. A novel flame-retardant acrylonitrile-butadiene-styrene system based on aluminum isobutylphosphinate and red phosphorus: Flame retardance, thermal degradation and pyrolysis behavior. Polym Degrad

Stabil 2014;109:184-193.

[27] Chen Y, Luo Y, Hu Z, Lin GP, Zhao B, Wang YZ, et al. An efficient halogen-free flame retardant for glass-fibre-reinforced poly(butylene terephthalate). Polym Degrad Stabil 2012;97(2):158-165.

[28] Schnabel W, Levchik GF, Wilkie CA, Jiang DD, Levchik SV. Thermal degradation of polystyrene, poly(1,4-butadiene) and copolymers of styrene and 1,4-butadiene irradiated under air or argon with ^{60}Co-γ-rays . Polym Degrad Stab 1999; 63(3):365-375.

[29] Torikai A, Kobatake T, Okisaki F. Photodegradation of Polystyrene Containing FlameRetardants: Effect of Chemical Structure of the Additives on the Efficiency of Degradation. J App Polym Sci 1998; 67(7): 1293-1300.

[30] Wang DY, Das A, Leuteritz A, Mahaling RN, Jehnichen D, Wagenknecht U, Heinrich G, et al. Structural characteristics and flammability of fire retarding EPDM/layered double hydroxide (LDH) nanocomposites. RSC Advances 2012;2(9):3927-3933.

[31] Xia YQ, Yang P, Miao Y, Zhang CL, Gu Y. Blends of sulfonated polysulfone/polysulfone/4,4’-diaminodiphenyl methane-based benzoxazine: multiphase structures and properties. Polym Int 2015; 64(1):118-125.